

## IN SILICO MOLECULAR DOCKING STUDIES ONNOVEL CHROMENO PYRIMIDINE ANALOGS FOR THEIR ANTI-MICROBIAL ACTIVITY

AmaturRoquia<sup>1</sup>

DrManoj Kumar<sup>2</sup>

<sup>1,2</sup>Department of Chemistry,  
Shri Venkateshwara University,  
Gujrala, India

### ABSTRACT

The aim of the study is to synthesize the novel chiral heterocyclic compounds which are biologically active and conduct docking studies to understand the various interactions between the synthesized compounds and micro organism. Pyrimidine is an important class of heterocyclic compound that are known to possess antimicrobial properties. 2H-chromenes are also known to possess antimicrobial properties. Chromenopyrimidines are compounds having both pyrimidines and 2H-chromenes rings. Hence, the synthesis of novel chromeno pyrimidine containing chloro, fluoro, trifluoromethyl groups have been carried. The synthesized compounds were characterized by <sup>1</sup>H NMR, <sup>13</sup>C NMR, <sup>19</sup>F NMR, FT-IR, GC-MS and elemental analysis. They were screened for their antibacterial activities against Gram-positive (Staphylococcus aureus, Bacillus subtilis), Gram negative (Escherichia coli, Pseudomonas aeruginosa) bacteria and anti-fungal activities against Aspergillus niger and Candida albicans by cup plate method. The mode of binding of the chromeno pyrimidine derivatives has been of interest because these compounds show activity against both bacteria and fungi. Flexible docking simulations were performed with a series of six chromeno pyrimidine derivatives. Binding preferences as well as the structural and energetic factors associated with them were studied, which suggest that the identified binding conformations of these inhibitors are reliable. Our studies suggest that these compounds having better binding interactions with microbial protein and hence, potentially, their therapeutic utility against microbes.

### General Terms

Molecular Docking, Molegro Virtual Docker (MVD), Multiple Linear Regression (MLR), Artificial Neural Network (ANN), Chromenopyrimidines, antibacterial, antifungal.

### 1. INTRODUCTION

Drug discovery has traditionally made progress by a combination of random screening and rational design [1]. In practice the synthetic chemists in the latter approach are often exasperated by the rarity of experimental data that defines the structure and properties of the biological target. The situation has changed with amalgamation of chemical and computational sciences. The advent in computing technology and exponential increase in the computing power has helped the chemists to define a new branch of chemistry "Computational Chemistry"[2]. The chemical methods which are well expressed mathematically can be

implemented for solving real world problem by designing such software and using them intelligently.

Despite these advances (and indeed partly because of them), drug discovery remains a difficult task, but at least we are now gathering together all the pieces of the puzzle, in terms of information, technologies and expertise[3,4].

Computer Aided Drug Design (CADD) employs computational methodologies to facilitate the drug discovery process. Through computations, one can predict binding interactions between a potential drug molecule and a receptor [5,6]. The physical properties of molecules can also be predicted enabling the focusing of experimental resource onto molecules that are more likely to make drug candidates.

Anti-bacterial and anti-fungal diseases are one of the major challenges for the medical science community. To control or cure these diseases they are frantically looking towards the chemical and biological scientific community for newer options of drugs. Growing consumption of various antibiotics for the treatment of microbial infections led to the appearance of multi-drug resistant (MDR) microbial pathogens.[7] Chemists, in specific, are the *de novo* designer of novel molecular entities which further are used by biologist (including microbiologists) for evaluating their biological profile and thereby suggesting probable molecular entities which can be used for probable treatment of various diseases. This studies deals with the use of computational tools for efficient and fast screening of organic molecules for generation of novel leads molecules which can be further synthesized and test for their inhibitory activity against HIV-1 infections. Molecular Modeling techniques including Docking and QSAR/QSPR [8-10] will be used to attain the goal.

Heterocyclic compounds are widely distributed in nature and are essential to life; they play a vital role in the metabolism of alliving cells. Heterocycles containing the chromene moiety and pyrimidineshows interesting features that make them an important target for combatting microorganisms. Chromenes, an important class of compound widely present in plant kingdom. [11]. They have gained recognition due to their contribution to biological activities such as anti-bacterial [12], antiviral [13], anti-cancer [14] and antimalarial [15] properties. The chromenes molecules lower toxicity [16,17].

Pyrimidine, a heterocyclic ring has structurally diverse synthetic derivatives [18] which are reported to show antimicrobial properties [19, 20].

## 2. MATERIAL AND METHODS

### 2.1 Molecular Structures

Newly fused chromene derivatives along with their biological activities were taken for docking studies. The molecular structures were drawn and geometrically optimized with MM2 force field using ChemDraw [21] and then exported to MolDock [22] where they were further prepared along with the proteins by the docking engine. The molecules were prepared by assigning bonds, bond orders, hybridization, charges, creating explicit hydrogens and flexible torsions in the ligand. The bond orders, the number of hydrogens attached to the atoms, and their hybridization were recognized and also the aromatic rings were detected. The charges were set according to the following scheme. The charge of the ligand atoms were set as follows: 0.5 charge for N atoms in  $-C(NH_2)_2$  HIS (ND1/NE2), 1.0 charge for N atoms in  $-N(CH_3)_2$ ,  $-(NH_3)$ , -0.5 charge for O atoms in  $-COO$ ,  $-SO_4$ ,  $-PO_2$ ,  $-PO_2^-$ , -0.66 charge for O atoms in  $-PO_3$ , -0.33 charge for O atoms in  $-SO_3$ , -1.0 charge for N atoms in  $-SO_2NH$ . The charge templates of the protein atoms were set as follows: 0.5 charge for N atoms in ARG (NH1/NH2), 1.0 charge for N atoms in LYS (N), -0.5 charges for O atoms in ASP (OD1/OD2) and GLU (OE1/OE2). The structure of microbial protein (PDB code 2V61) was obtained from Protein Data Bank [Research Collaboratory for Structural Bioinformatics (RCSB) [23].

### 2.2 Docking Simulations

MolDock software is based on a new heuristic search algorithm that combines differential evolution with a cavity prediction algorithm [24]. Previously, differential evolution (DE) has been successfully applied to molecular docking [25, 26]. Fast and accurate identification of potential binding modes (poses) can be achieved using the predicted cavities during the search process. The MolDock docking scoring function is based on a piecewise linear potential (PLP) introduced by Gehlhaar et al. [27, 28] and further extended in GEMDOCK by Yang and Chen [29]. Here, the docking scoring function takes hydrogen bond directionality into account. EPLP is a piecewise linear potential using two different sets of parameters: one for approximating the steric (van der Waals) term between atoms and the other stronger potential for hydrogen bonds. Moreover, a re-ranking procedure has been applied to the highest ranked poses to further increase the docking accuracy. On an average, 10 docking runs were made to obtain a high docking accuracy. Only the ligand properties are represented in the individuals, because the protein remained rigid during the docking process. Mol-Dock automatically identifies potential binding sites (cavities) using a flexible cavity detection algorithm as there is no dependence on the orientation of the target molecule and an arbitrary number of directions can be used. The fitness of a candidate solution is

derived from the docking scoring function,  $E_{score}$  and is defined by the following energy terms

$$E_{score} = E_{inter} + E_{intra}$$

The summation runs over all heavy atoms in the ligand and all heavy atoms in the protein, including any cofactor atoms and water molecule atoms that might be present. The second term describes the electrostatic interactions between charged atoms.  $E_{intra}$  is the internal energy of the ligand:

$$E_{intra} = \sum_{i \in \text{ligand}} \sum_{j \in \text{ligand}} E_{PLP}(r_{ij}) + \sum_{\text{flexible bonds}} A [1 - \cos(m * \theta - \theta_0)] + E_{clash}$$

The double summation is between all atom pairs in the ligand, excluding atom pairs that are connected by two bonds or less. The second term is a torsional energy term, parametrized according to the hybridization types of the bonded atoms.  $h$  is the torsional angle of the bond. The last term,  $E_{clash}$ , assigns a penalty of 1,000 if the distance between two atoms (more than two bonds apart) is less than  $2.0 \text{ \AA}$ . Thus, the Eclash term punishes the infeasible ligand conformations.

### 2.3 Hardware and software

Molegro Virtual Docker 2007.2.2 [22] was run on a windows XP based pentium IV 2.66 GHz PC (with 512 MB of memory).

## 3. RESULTS AND DISCUSSION

### 3.1 Molecular Docking

Our specific aims for the present study were threefold: Firstly, to estimate the relative protein-ligand energy in the context of structure-based drug design (SBDD) using available data, secondly, to understand the variations in protein-ligand interaction of results related to structural and energetic correlations, as derived from the simulations. Thirdly find correlation between various docking parameters with anti-bacterial/anti-fungal activity. The chemical structures of 6 newly chromene derivatives are given in Table 1 along with their antibacterial *S.aureus*(A1), *B.subtilis*(A2), *E.Coli*(A3), *P.aeruginosin*(A4), and antifungal activities *niger*(B1), *Albicans*(B2) and the types of substituent as X and Y. X represents the substitution on the Chromene ring, Y represents substitution on the pyrimidine ring.

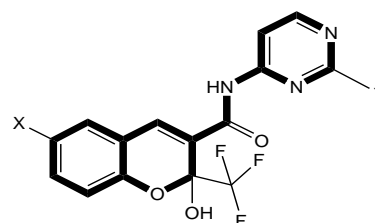


**Table 1: Substituent X on chromene ring and Y on pyrimidine ring with the biological activity against gram Positive, gram negative bacteria and fungus.**

no.	X	Y	Gram (+)ve bacteria		Gram (-)ve bacteria		Fungus	
			A1	A2	A3	A4	B1	B2
			50	50	50	50	50	50
			μg/ mL	μg/ mL	μg/ mL	μg/ mL	μg/ mL	μg/ mL
6a1	Cl	F	12	10	11	10	11	11
6a2	Cl	CF <sub>3</sub>	18	19	16	18	11	10
6b1	CF <sub>3</sub>	H	15	14	13	12	14	16
6b2	CF <sub>3</sub>	F	17	18	17	17	16	17
6b3	CF <sub>3</sub>	Cl	18	20	18	18	17	20
6c2	F	CF <sub>3</sub>	19	20	17	18	17	19

Table 2 records the protein ligand energy ( $E_{P-L}$ ) in kJ/mol, Rerank score (both in arbitrary energy units), steric energy, no. of torsions ( $\tau$ ), vanderwaalVdW ( $LJ_{12-6}$ ) interactions and no. of halogen(X).

No.	$E_{P-L}$	Rerank Score	Steric Energy	$\tau$	VdW ( $LJ_{12-6}$ )	X
6a1	-123.64	-19.72	-123.64	3	67.98	5
6a2	-125.79	-68.85	-125.79	4	-18.46	7
6b1	-128.47	-37.70	-128.42	3	57.39	6
6b2	-131.39	-39.30	-131.33	4	57.15	7
6b3	-129.30	-39.18	-129.30	4	56.35	7
6c2	-151.61	-52.74	-148.46	4	58.67	7

An important application of the protein ligand energy is supposed to be the best choice while identifying the best binder to a given target in a varied ligand dataset. The reranked scores predicted the protein-ligand energy in the range of -19.725 to -68.858 kJ/mol. The binding of these compounds occur at a catalytic and allosteric site, which has an inner hydrophobic core stacked mainly with TYR398, TYR326 amino acid residues. The other amino acids involved in the hydrophobic interactions with these inhibitors are PHE168, CYS172, PRO102, PRO104, TRP119, LEU164, PHE103, GLN206, ILE199 [30, 31]. Important differences occur in the conformation of amino acid residues that form the binding pocket [32]. These crystal structures provide valuable clues for designing new inhibitors by providing deep knowledge about the pattern of interaction in the binding pocket [33].

### 3.2 Validation of the docking method:

For the present studies, we have selected a protein (PDB code 2V61)[34] containing the ligand C18. The X-ray crystallographic structure of C18 refined at 1.7 Å resolution has been considered for the docking studies. The ligand was extracted from the complex (2V61) and redocked using flexible docking simulations into its original structure of microbial protein. The starting coordinates of the microbial complex (2V61) were imported from the Protein Data Bank (www.rcsb.org). Bond orders, charges, flexible torsions were assigned to them, the side chains were protonated and the bond flexibility of the ligands was checked. The receptor (protein molecule) was minimized locally as well as globally using Nedler-Mead simplex algorithm. Potential binding sites were identified using theMolDock optimizer. MolDock Grid with 30Å resolution was used for docking. The following parameters: No. of runs = 20, population size = 100, crossover rate = 0.9, scaling factor = 0.5, and max iterations = 4000, termination = RMSD based were fixed. It was followed by pose clustering so that the best-scoring pose was not missed out. Five top scoring poses were returned. Fitness evaluation was done by MolDock [Grid] scoring functions (grid resolution = 0.30) based on PLP and GEMDOCK and were again reranked to increase the docking accuracy. This was followed by simple docking using differential evolution algorithm, so that diverse poses were returned. A satisfactory agreement was obtained for the redocked ligand and the alignment of the ligand within the X-ray crystal coordinates (0.560 Å) as shown in figure 1.

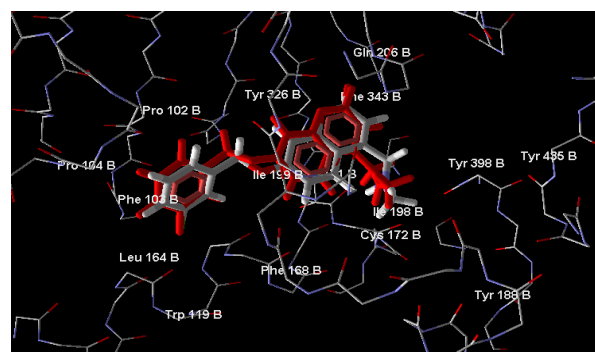
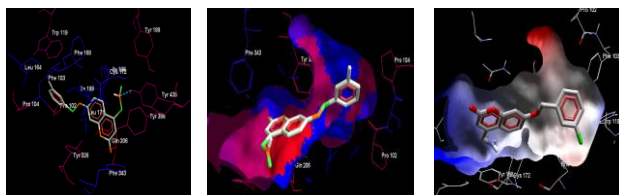


**Figure 1:** Superimposed binding orientation of docked conformer (red) and most stable ligand (CPK) within the active binding site region of 2V61.

Hydrogen bond interaction (Figure 2-a) is observed with the amino acid residue TYR435 ( $E_{H-bond} = -2.5$  kJ and bond length = 2.965). The hydrogen bonding strength helps in enhancing the binding efficacy. The hydrophobic (Figure 2-b) as well as the electrostatic (Figure 2-c) contour map shows favorable interactions with the binding pocket. The hydrophobic or the lyophilic environment of the protein are mainly attributed to the interactions of the amino acid residues PHE343, TYR188, TYR435, TYR326, TYR398, PHE168, CYS172, PRO102, PRO104, TRP119, LEU164, PHE103, GLN206, ILE199 and ILE198 with the ligand.

Benzene group of C18 are involved in hydrophobic interactions with the surrounding amino acid residues and  $\text{CH}_2\text{NHCH}_2$  group attached with chromene ring are involved in hydrophilic interactions. The electrostatic contour map depicts the ionic and the polar interactions between the protein and the ligand molecules. The  $\text{CH}_2\text{NHCH}_2$  group inserts into blue part and chlorine inserts into grey part which is near to red part. The positive valued molecular electrostatic potential (MESP) region (blue) is predominant and accounts for the nucleophilic substitution.



2-a

2-b

2-c

**Figure 2-a:** Hydrogen Bond Interactions Shown by Dotted Lines (H-bond Interactions is Observed with TYR435 ( $E_{\text{H-bond}} = -2.5$  kJ and bond length = 2.965).

**Figure 2-b:** Hydrophobic Interactions (Hydrophobic Interactions are Depicted by Blue and Hydrophilic Interactions are Depicted by Red) and

**Figure 2-c :** Electrostatic Interactions (Positive Interactions are Depicted by Blue and Negative Interactions are Depicted by Red) of the C18/protein.

### 3.3 Docking of Newly Fused ChromenoPyrimidine Molecules

Docking of the molecular data set after the validation of the docking method using C18, a dataset of 6 molecules belonging to newly fused chromeno pyrimidine derivatives with varied activity range (4.0–8.52) were docked into the same coordinates of the crystal structure. The same docking protocol was used for all the docking calculations. 6a2 showed good fit with the reference ligand C18. The docked 3D-structures of newly fused chromeno pyrimidine derivatives were scored, reranked and then compared with the X-ray crystallographic structure of C18. The beauty of this series was that all the compounds share a basic common pattern. The result demonstrates that the docking simulation can dock these newly fused chromeno pyrimidine inhibitors back into the protein allosteric binding site very well as per expectation that similar compounds bind in a similar way. Although, most of the compounds prefer one single binding position deeply buried in the allosteric binding pocket multiple binding orientations were also observed.

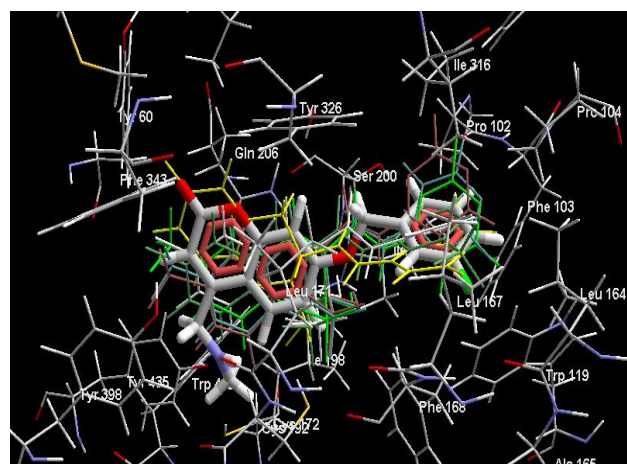


**Figure 3:** Docked Conformation of C18 (CPK) with Best Fit Analogues of newly fused chromeno pyrimidine analogues (Cpd. Nos. 6a1 (white), 6a2 (green), 6b1 (blue), 6b2 (brown), 6b3 (light green) and 6c2 (yellow).

The stereochemical changes produced due to receptor-inhibitor interaction in the protein binding pocket play a crucial role in determining the therapeutic properties of the inhibitor molecule.

### 3.4 Hydrogen Bond Interaction of Newly Fused Chromeno Pyrimidine Molecules

The  $\text{CF}_3$  moiety attached at pyrimidine ring orients itself in a way to have closer interaction with LEU164, TRP119, PRO102, PRO104 and PHE103. While the chlorine attached at chromeno ring orients itself in a way to have closer interaction with TYR398 and PHE343 of newly fused chromenopyrimidine derivatives have moderate values of protein-ligand energy. As the newly fused chromeno pyrimidine compounds have the same basic structure, as expected, similar interactions are observed. Hydrogen bonding interaction was observed between carbon of the chromeno ring forms hydrogen bond ( $E_{\text{H-bond}} = -2.5$  kJ) with oxygen of TYR435 amino acid residues given in table-2. Also, all compounds are weakly bound as compared to C18.

Table-2 : Hydrogen bond energy and hydrogen bond length with amino acid residue TYR435 with respect to microbial protein.

Comp No.	$E_{\text{H-bond}}$ (KJ)	Bond length(Å)
6a1	-2.5	3.439
6a2	-2.5	3.154
6b1	-2.5	3.416
6b2	-2.5	3.295
6b3	-2.5	3.492
6c2	-2.5	4.697

All the newly fused chromeno pyrimidine ring shows hydrogen bond interaction with amino acid residue TYR435 as shown in figure 3.

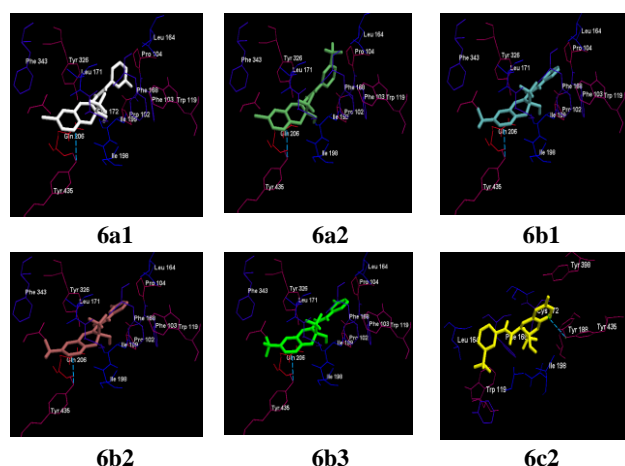


Fig 3: Hydrogen bond interaction of newly fused chromenopyrimidine ring with amino acid residue TYR435.

### 3.5 Electrostatic Interaction of Newly Fused ChromenoPyrimidine Molecules

The surface map of the binding pocket also showed favorable electrostatic interactions with the ligand (Fig. 4). Electrostatics of molecules provide a highly informative means of characterizing the essential electronic features of inhibitors and their stereoelectronic complementarities with the receptor site on the basis of ionic and polar interactions between the host and the guest. As expected the major role was played by a chromene ring moiety present in the structure. As the contour map exhibiting blue color indicated more positive charge i.e. a nucleophilic attachment would be favorable for electronic interactions. The electrostatic interaction was stabilized by stacking type interaction with chromene and pyrimidine ring located at the receptor site, the chromene ring shows  $\pi$ - $\pi$  interaction with TYR398 and pyrimidine ring shows  $\pi$ - $\pi$  interaction with TYR326.

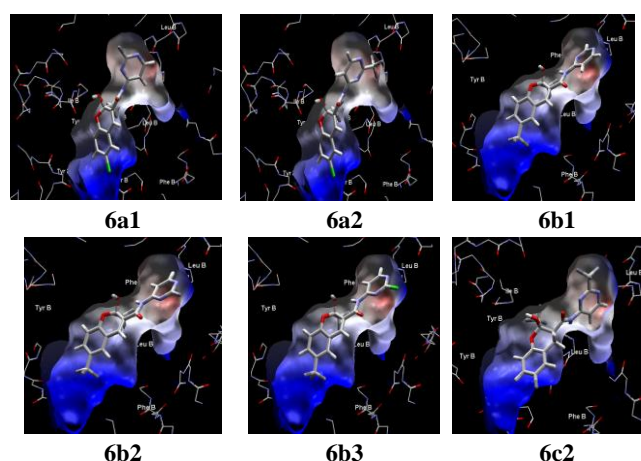


Fig 4: Electrostatic interaction of newly fused chromeno pyrimidine ring

### 3.6 Hydrophobic interaction of Newly fused ChromenoPyrimidine Molecules

The newly fused chromeno pyrimidine compounds seemed to be stabilized by extensive hydrophobic interactions (Fig. 5). The major contributor to the hydrophobicity seemed to be the pyrimidine ring and the halogen attached to chromeno ring. The aromatic moieties of the amino acid residues converge at the inner side of the binding cavity. The chromene ring inserts into red part shows hydrophilic interaction with amino acid residues. The chromene ring shows  $\pi$ - $\pi$  interaction with TYR398 and pyrimidine ring shows  $\pi$ - $\pi$  interaction with TYR326, which gives extra stability to the ligand to fit in the pocket.

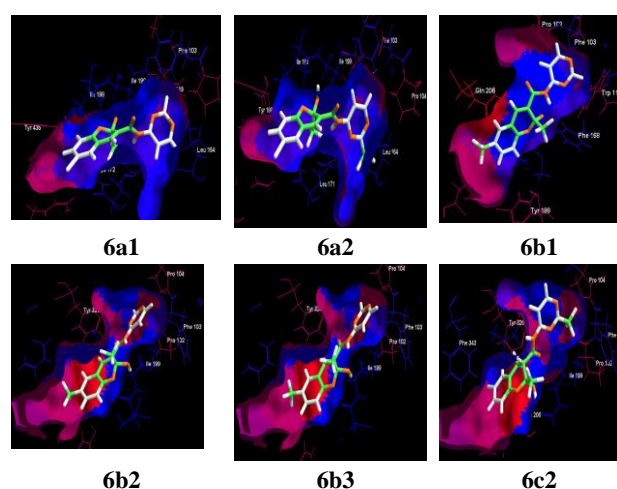


Fig 5: Hydrophobic interaction of newly fused chromeno pyrimidine ring

### 3.7 Correlation between various docking parameters and microbial activity

The protein ligand energy is supposed to be the best choice while identifying the best binder to a given target in a varied ligand dataset. The reranked scores predicted the protein-ligand energy in the range of -19.43 to -25.27 kJ/mol.

#### 3.7.1 Multiple linear regression technique (MLR) and Artificial Neural Network analyses

Various models were created using multiple linear regression technique (MLR) [35-42] and artificial neural networks (ANN) [35-42] using in-built data analyzer. Biological activity was taken as the dependent variable. The auto generated random seed used in the model training was 1265312701. In these equations,  $n$  is the number of compounds,  $r^2$  is the correlation coefficient. Multiple linear regression technique (MLR) The best model relating biological activity with the various parameters were derived using MLR and ANN for *S.aureus*(A1),

B.subtilis(A2),E.Coli(A3), P. aeruginosin(A4), niger(B1), Albicans(B2) presented in table-3.

Table 3: Correlation coefficient ( $R^2$ ) between the various docking parameters and antibacterial/antifungal activity.

	$E_{p-L}$		Rerank Score		Steric	
	MLR ( $R^2$ )	ANN ( $R^2$ )	MLR ( $R^2$ )	ANN ( $R^2$ )	MLR ( $R^2$ )	ANN ( $R^2$ )
<b>A1</b>	0.33	0.33	0.62	0.90	0.35	0.60
<b>A2</b>	0.26	0.57	0.56	0.86	0.28	0.60
<b>A3</b>	0.22	0.58	0.36	0.70	0.24	0.59
<b>A4</b>	0.22	0.37	0.57	0.78	0.23	0.38
<b>B1</b>	0.42	0.93	3.19	0.34	0.46	0.94
<b>B2</b>	0.35	0.86	0.01	0.45	0.38	0.87

Table 3 continued.....

	T		VdW ( $LJ_{12-6}$ )		X	
	MLR ( $R^2$ )	ANN ( $R^2$ )	MLR ( $R^2$ )	ANN ( $R^2$ )	MLR ( $R^2$ )	ANN ( $R^2$ )
<b>A1</b>	0.79	0.79	0.15	0.72	0.95	0.96
<b>A2</b>	0.83	0.47	0.14	0.73	0.98	0.98
<b>A3</b>	0.89	0.89	0.06	0.37	0.95	0.96
<b>A4</b>	0.94	0.94	0.18	0.63	0.97	0.99
<b>B1</b>	0.23	0.23	0.24	0.35	0.34	0.36
<b>B2</b>	0.11	0.11	0.35	0.47	0.21	0.27

Figure 6 shows the graphical representation for various docking parameters and anti-bacterial/antifungal activity in terms of correlation coefficient.

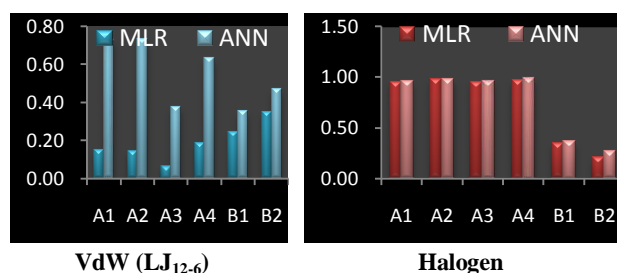
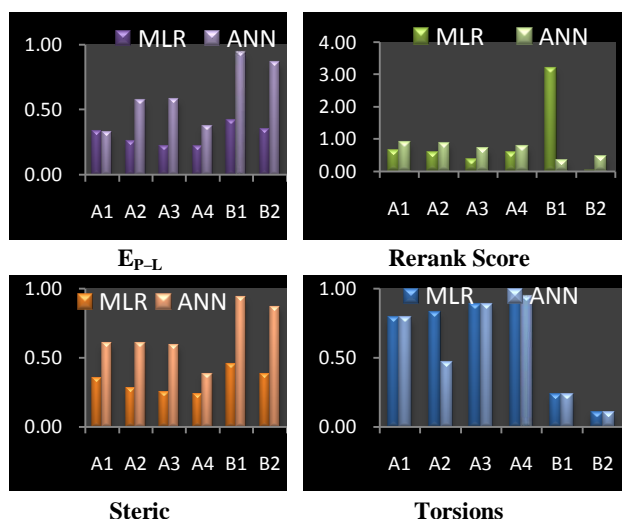


Fig 6: Bar graph shows correlation coefficient using MLR and ANN analyses between the various docking parameters and antibacterial/anti-fungal activity.

The results derived from MLR and ANN analyses for protein ligand energy shows that ANN performs better than MLR. While compare anti bacterial and antifungal activity the ANN performs better for antifungal activity. In case of rerank score ANN performs better than MLR. But ANN performs better for antibacterial activity. In case of steric ANN performs better for anti fungal activity. No. of torsions,vanderwaal energy and halogen are well behaved in terms of ANN in the antibacterial activity. Among all the correlation P. aeruginosin antibacterial activity well correlates with halogen using ANN analyses. This shows that halogens are better for enhancing the activity against microbial protein.

Artificial neural networks (ANN) the algorithm used for training NN model was backpropagation method. Using the same random seed, following parameters were fixed: max training epoch =1,500, learning rate = 0.50, output learning rate = 0.30, momentum = 0.20, no. of neurons in the first hidden layer = 1, initial weight ( $\pm$ ) = 0.30. Altering the above parameters of neural network did not yield any significant change in the value of  $r^2$ . The above statistical analyses suggest the robustness of the docking procedure adopted herein and the results obtained can be validated by Fig. 6 (correlating biological activity with the various docking parameters).

Although they showed a good geometric fit they yielded a lower value of protein-ligand energy. This suggests some complexity in the binding interaction, which might be related to protein flexibility or some modified interaction upon binding.

Our findings suggest that newly fused chromenopyrimidine derivatives interacting more closely with these conserved residues TYR435, TYR326 and TYR398 in the microbial pocket and have better protein-ligand energy and targeting these conserved amino acids for drug-design purposes may yield drugs that are effective in escaping mutations. Hence, these scaffolds can be used as starting point in the design and synthesis of novel and potential hit compounds.

#### 4. CONCLUSIONS

Novel chromenopyrimidines were synthesized using a simple multi-step strategy in good yields. The synthesized compounds were well characterized and tested for their antibacterial and antifungal activities. The fluoro-substituted compounds showed the greatest activities. These results give an insight into the structure-property relationships, which are tremendously important for the design of further new antimicrobial compounds.

Docking studies were performed on newly fused Chromeno Pyrimidine analogues to evaluate their stereochemical compatibility with the microbial inhibitor binding pocket. Coordinates of the redocked ligand pose matched reasonably to the X-ray crystal coordinates (PDB code: 2V61). On the basis of this, reliable binding modes and protein-ligand energy were obtained for the new analogues of chromeno ring are active and are good precursors for the microbes. As the protein considered here, had limited side chain flexibility, we were able to derive better binding preferences. The electrostatic interaction of the halogen suggested that the positive valued molecular electrostatic potential (MESP) region (blue) is predominant and accounts for the nucleophilic substitution. Though the hydrogen bond interaction with amino acid residue TYR435 are little weak as compared to reference ligand. The derivatives shows  $\pi$ - $\pi$  interaction with TYR398 and pyrimidine ring shows  $\pi$ - $\pi$  interaction with TYR326, which gives extra stability to the ligand to fit in the pocket and these scaffolds would be a better hit in the drug discovery pipeline. Thus, novel compounds having better binding interactions with microbial protein.

#### 5. ACKNOWLEDGMENTS

Our special thanks to Dr. Nilanjana Jain for helping in the docking studies of chromene derivatives.

#### 6. REFERENCES

- [1] Zhuang X., Lu C., Acta Pharm Sin B., (2016), 6(5), 430-440.
- [2] Liu J., J Chem Phys., (2016) 145(20), 204105.
- [3] Öster L., Tapani S., Xue Y., Käck H., Drug Discov Today., (2015) 20(9), 1104-1111.
- [4] Ding C.B., Zhao Y., Zhang J.P., Peng Z.G., Song D.Q., Jiang J.D., Int J Mol Med., (2015) 35(3), 791-797.
- [5] Brown F.K., Sherer E.C., Johnson S.A., Holloway M.K., Sherborne B.S., J Comput Aided Mol Des., (2016), 16, 79-81.
- [6] Tu J., Li J.J., Shan Z.J., Zhai H.L., Antiviral Res. (2016), 30303-5.
- [7] Kharb,R., Tyagi,M., and Sharma,A. K.,Der Pharma Chem., (2014) . 6, 298-320.
- [8] Qian Y., Liang Y., Liu W., Liang G., J. Mol Graph Model., (2016) 71, 88-95.
- [9] Miliutina M., Ejaz S.A., Khan S.U., Iaroshenko V.O., Villinger A., Iqbal J., Langer P., Eur J Med Chem., (2016), 126, 408-420.
- [10] Raskevicius V., Kairys V., CurrComput Aided Drug Des. (2016) Nov 29
- [11] Murray, R. D., Mendez, J., and Brown, S. A., 1982 The Natural Coumarins: Occurrence, Chemistry and Biochemistry. Hoboken, New Jersey, United States: John Wiley & Sons..
- [12] Prasad, M. R., Prashanth, J., Shilpa, K. and Kishore, D. P.ChemInform, (2007) 38, 40.
- [13] Aly, H. M., Saleh, N. M. and Elhady, H. Eur. J. Med. Chem., (2011) 46, 9, 4566-4572.
- [14] Ashalatha, B. V., Narayana, B., Raj, K. K. V. and Kumari, N.Eur. J. Med. Chem, (2007) 42, 719-728.
- [15] George, T., Kaul, C., Gmwal, R. S. and Tahilramani, R.J. Med. Chem, (1971) 14, 913-915.
- [16] Bruno, O., Brullo, C., Ranise, A., Schenone, S., Bondavalli, F., Barocelli, E., Ballabeni, V., Chiavarini, M., Tognolini, M. and Impicciatore, M.Bioorg Med Chem Lett, (2001) 11, 11, 1397-1400.
- [17] Russell, R. K., Press, J. B., Rampulla, R., McNally, J. J., Falotico, R., Keiser, J., Bright, D. and Tobia, A.J. Med. Chem., (1988) 31, 9, 1786-1793.
- [18] Liu, H., Wang, H.-Q. and Liu, Z.-J.Bioorg. Med. Chem. Lett., (2007) 17, 8, 2203-2209.
- [19] Wang, J.-M., Asami, T., Yoshida, S. and Murofushi, N.Biosci. Biotechnol. Biochem., (2001) 65, 4, 817-822.
- [20] Acosta, P., Insuasty, B., Ortiz, A., Abonia, R., Sortino, M., Zacchino, S. A. and Quiroga, J. Arab. J. Chem., (2015).
- [21] [www.cambridgesoft.com/support/](http://www.cambridgesoft.com/support/)
- [22] <http://www.molegro.com> (free trial version)
- [23] Berman H.M., Westbrook J., Feng Z., Gilliland G., Bhat T.N., Weissig H., Shindyalov I.N., Bourne P.E.,Nucleic Acids Res (2000) 28, 235-239.
- [24] Thomsen R., Christensen M.H., J Med Chem (2006) 49, 3315-3326.
- [25] Storn R, Price K. (1995) Differential evolution – a simple and efficient adaptive scheme for global optimization over continuous spaces. Technical Report, International Computer Science Institute, Berkley, CA
- [26] Thomsen R. (2003) Flexible ligand docking using differential evolution. In: Proceedings of the 2003 congress on evolutionary computation, vol 4, pp 2354-2361.
- [27] Gehlhaar D.K., Verkhivker G., Rejto P.A., Fogel D.B., Fogel L.J., Freer S.T. (1995) Docking conformationally flexible small molecules into a protein binding site through evolutionary programming. In: Proceedings of the fourth international conference on evolutionary programming, pp 615-627.
- [28] Gehlhaar D.K., Bouzida D., Rejto P.A. (1998) Fully automated and rapid flexible docking of inhibitors covalently bound to serine proteases. In: Proceedings of the seventh international conference on evolutionary programming, pp 449-461.
- [29] Yang J.M., Chen C.C.,Proteins, (2004) 55, 288-293.
- [30] Mager P.P.,Med Res Rev, (1997) 17, 235-239.

- [31] Tantillo C, Ding J, Jacobo-Molina A, Nanni RG, Boyer PL, Hughes SH, Pauwels R, Andries K, Janssen PA, Arnold E (1994) *J MolBiol* 243:369
- [32] Ding J., Das K., Moereels H., Koymans L., Andries K., Janssen P.A., Hughes S.H., Arnold E., *Nat StructBiol*(1995) 2, 407-413.
- [33] Barreca M.L., Rao A., De Luca L., Zappala M., Monforte A.M., Maga G., Pannecouque C., Balzarini J., De Clercq E., Chimirri A., Monforte P., *J Med Chem*(2005) 48, 3433-3439.
- [34] <http://www.rcsb.org/pdb/explore/explore.do?structureId=2v61>.
- [35] Jain (Pancholi) N., Gupta S., Sapre N. and Sapre N. S., *RSC Adv.* (2015) 5, 14814-14827.
- [36] Pancholi N., Sapre N. S., *Asian J. Chem.* (2007) 19, 2, 1251-1261.
- [37] Sapre N.S., Pancholi N., Gupta S., Sikarwar A. and Sapre N., *J. Chem. Sci.* (2007) 119, 6,625-630.
- [38] Sapre N. S., Pancholi N. and Gupta S., *Int. Elec. J. Mol. Des.* (2008) 7, 3, 55-67.
- [39] Sapre N. S., Pancholi N. Gupta S., and Sapre N., *RSC Adv.* (2013) 3, 10442-10451.
- [40] Jain (Pancholi) N., Gupta S., Sapre N. and Sapre N. S., *Mol. Biosys.* (2014) 10, 313-325.
- [41] Sapre N. S., Gupta S. Pancholi N. and Sapre N., *J.Mol.Mod.* (2008) 14, 1009-1021.
- [42] Sapre N. S., Pancholi N. Gupta S., and Sapre N., *J. Comp.Chem* (2009) 29, 11, 1700-1706.

